ANS MC2015 - Joint International Conference on Mathematics and Computation (M&C), Supercomputing in Nuclear Applications (SNA) and the Monte Carlo (MC) Method · Nashville, Tennessee · April 19–23, 2015, on CD-ROM, American Nuclear Society, LaGrange Park, IL (2015)

A NON-NEGATIVE, NON-LINEAR, PETROV-GALERKIN METHOD FOR BILINEAR DISCONTINUOUS DIFFERENCING OF THE S_N EQUATIONS

Peter G. Maginot, Jean C. Ragusa*, and Jim E. Morel
Department of Nuclear Engineering
Texas A&M University
3133 TAMU, College Station, TX 77843
pmaginot@tamu.edu; jean.ragusa@tamu.edu; morel@tamu.edu

ABSTRACT

We have developed a new, non-negative, non-linear, Petrov-Galerkin discontinuous finite element method (NNPGDFEM), for use in conjunction with Galerkin bilinear discontinuous (BLD) finite element differencing of the 2-D Cartesian geometry S_N equations for quadrilaterals on an unstructured mesh. This work is an extension of the idea that drove our previous development of a NNPGDFEM for use with linear discontinuous (LD) differencing of the 2-D Cartesian geometry S_N equations for rectangular mesh cells. We present the theory and equations that describe the new method. Additionally, we numerically compare the accuracy of our proposed method to the accuracy of the BLD scheme (without lumping) and the subcell corner balance method (equivalent to a "fully" lumped bilinear discontinuous scheme) for a test problem in which the BLD solution contains negative angular flux solutions

Key Words: Radiation transport, DFEM, non-negative, bilinear, quadrilaterals

1 INTRODUCTION

Discontinuous finite element method (DFEM) spatial discretizations of the S_N neutron transport equation and S_N thermal radiative transfer equations can result in negative angular flux and negative angular intensity solutions. These negative solutions are non-physical, but inherent to the mathematics that define the radiation spatial differencing scheme. Several researchers have examined several different methods (matrix lumping [1], fix-ups [2], and strictly non-negative solution representations [3]) that inhibit or eliminate the negativities of the linear discontinuous (LD) finite element scheme on a variety of spatial mesh cell types (slab, rectangular, triangular, ...), for the S_N neutron transport equation. However, Adams showed that LD does not maintain the neutronics thick diffusion limit on quadrilaterals [1]. We are interested in accurate methods for radiative transfer on quadrilaterals, therefore we seek methods that can maintain the radiative transfer equilibrium diffusion limit on quadrilaterals. If a radiative transfer spatial discretization is to maintain the equilibrium diffusion limit, its neutron transport analog must preserve the the thick diffusion limit. As a first step towards accurate methods for radiative transfer on quadrilaterals, we thus seek non-negative, bilinear discontinuous (BLD) finite element spatial discretizations of the neutron transport equation on quadrilaterals.

*Corresponding author

The Galerkin BLD spatial discretization for quadrilaterals, more commonly referred to as unlumped bilinear discontinuous (UBLD) yields negative angular flux solutions for spatial cells with glancing radiation incidence and/or large optical thickness [1]. To our knowledge, only matrix lumping has been considered in an attempt to inhibit negative angular flux solutions of BLD spatial discretizations. While more common forms of matrix lumping, such as mass matrix or combination mass and surface matrix lumping, inhibit negative angular flux solutions, they do not guarantee a strictly non-negative BLD angular flux solution [1]. Wareing, et. al, derived the fully lumped BLD (FLBLD) scheme [4], that uses additional manipulations of the UBLD equations to yield angular flux solutions that are strictly non-negative. Unfortunately, Adams demonstrated that FLBLD, which is equivalent to the subcell balance method on rectangles, is less accurate than the unlumped BLD (UBLD) scheme for spatial mesh cells of thin and intermediate thicknesses [5].

In [3], we developed a non-negative, non-linear Petrov-Galerkin DFEM for use in conjunction with LD spatial differencing of the S_N equations in slab and rectangular Cartesian geometry. In this paper, will extend the main idea of [3] to create a non-negative, non-linear Petrov-Galerkin DFEM to be used with UBLD spatial differencing on unstructured quadrilaterals. The remainder of this paper is divided as follows: a description and derivation of our new, bilinear consistent set-to-zero (BCSZ) Petrov-Galerkin scheme is given in Section 2, computational results demonstrating the strictly positive nature of BCSZ and its improved accuracy relative to UBLD and FLBLD are given in Section 3, and conclusions are given in Section 4.

2 DERIVATION

We begin by first considering the 2-D Cartesian discrete ordinates transport equation:

$$\vec{\Omega}_d \cdot \nabla\psi(x,y,\vec{\Omega}_d) + \sigma_t(x,y)\psi(x,y,\vec{\Omega}_d) = S_d(x,y)\,, \tag{1}$$

where $\vec{\Omega}_d$ is the neutron direction, $\psi(x,y,\vec{\Omega}_d)$ is the angular flux $[n/(cm^s\ sec\ ster)]$, $\sigma_t(x,y)$ is the total interaction cross section $[cm^{-1}]$, and $S_d(x,y)$ is the total source (scattering + fixed sources) in direction $\vec{\Omega}_d$. Following the standard Galerkin procedure and taking the moment of Eq. (1) with respect to basis function $B_i(x,y)$ by first multiplying by $B_i(x,y)$ and then integrating over spatial cell K. Assuming cell-wise constant σ_t, we have:

$$\int_K B_i(x,y)\left[\vec{\Omega}_d \cdot \nabla\psi(x,y,\vec{\Omega}_d) + \sigma_t\psi(x,y,\vec{\Omega}_d)\right]\,dxdy = \int_R B_i(x,y)S(x,y)\,dxdy\,. \tag{2}$$

Using integration by parts Eq. (2) becomes:

$$(\vec{\Omega}_d\cdot\vec{n})\oint_R B_i(x,y)\psi(x,y,\vec{\Omega}_d)\,dS - \int_R \psi(x,y,\vec{\Omega}_d)\left[\vec{\Omega}\cdot(\nabla_{xy}B_i(x,y))\right]dxdy + \sigma_t\int_R B_i(x,y)\psi(x,y,\vec{\Omega}_d)\,dxdy\,. \tag{3}$$

We now define a reference element mapping in Fig. 1: that transforms from a reference point (s,t), $s\in[-1,1]$ $t\in[-1,1]$, to a physical point (x,y) such that:

$$x = x_0B_0(s,t) + x_1B_1(s,t) + x_2B_2(s,t) + x_3B_3(s,t) \tag{4}$$

$$y = y_0B_0(s,t) + y_1B_1(s,t) + y_2B_2(s,t) + y_3B_3(s,t)\,. \tag{5}$$

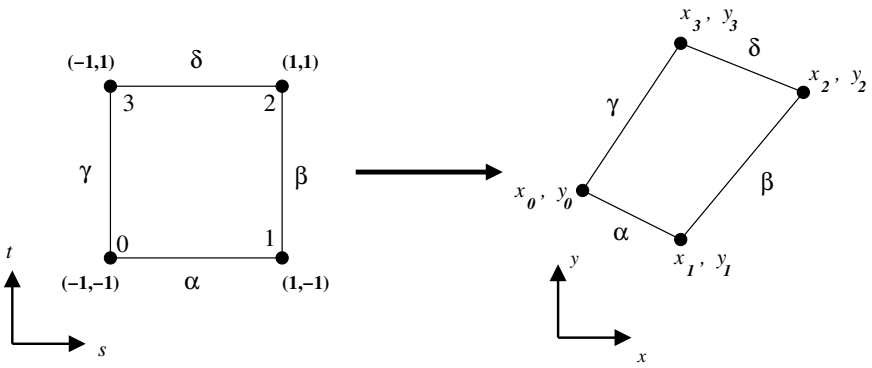

Figure 1. Reference element mapping.

Our basis function are the bilinear Lagrange interpolatory functions defined on the reference element:

$$B_0(s,t) = \frac{1-s}{2}\frac{1-t}{2} \tag{6a}$$

$$B_1(s,t) = \frac{s+1}{2}\frac{1-t}{2} \tag{6b}$$

$$B_2(s,t) = \frac{s+1}{2}\frac{t+1}{2} \tag{6c}$$

$$B_3(s,t) = \frac{1-s}{2}\frac{t+1}{2}\,. \tag{6d}$$

For every direction $\vec{\Omega}_d$, the four, exact, bilinear moment equations are:

$$(\vec{\Omega}\cdot\vec{n}_\alpha)\psi_{1,\alpha} + (\vec{\Omega}\cdot\vec{n}_\beta)\psi_{1,\beta} + (\vec{\Omega}\cdot\vec{n}_\delta)\psi_{1,\delta} + (\vec{\Omega}\cdot\vec{n}_\gamma)\psi_{1,\gamma} - \mu\psi_{1,\mu} - \eta\psi_{1,\eta} + \sigma_t\psi_{1,M} = S_{1,M} \tag{7a}$$

$$(\vec{\Omega}\cdot\vec{n}_\alpha)\psi_{2,\alpha} + (\vec{\Omega}\cdot\vec{n}_\beta)\psi_{2,\beta} + (\vec{\Omega}\cdot\vec{n}_\delta)\psi_{2,\delta} + (\vec{\Omega}\cdot\vec{n}_\gamma)\psi_{2,\gamma} - \mu\psi_{2,\mu} - \eta\psi_{2,\eta} + \sigma_t\psi_{2,M} = S_{2,M} \tag{7b}$$

$$(\vec{\Omega}\cdot\vec{n}_\alpha)\psi_{3,\alpha} + (\vec{\Omega}\cdot\vec{n}_\beta)\psi_{3,\beta} + (\vec{\Omega}\cdot\vec{n}_\delta)\psi_{3,\delta} + (\vec{\Omega}\cdot\vec{n}_\gamma)\psi_{3,\gamma} - \mu\psi_{3,\mu} - \eta\psi_{3,\eta} + \sigma_t\psi_{3,M} = S_{3,M} \tag{7c}$$

$$(\vec{\Omega}\cdot\vec{n}_\alpha)\psi_{4,\alpha} + (\vec{\Omega}\cdot\vec{n}_\beta)\psi_{4,\beta} + (\vec{\Omega}\cdot\vec{n}_\delta)\psi_{4,\delta} + (\vec{\Omega}\cdot\vec{n}_\gamma)\psi_{4,\gamma} - \mu\psi_{4,\mu} - \eta\psi_{4,\eta} + \sigma_t\psi_{4,M} = S_{4,M}\,, \tag{7d}$$

where we have defined the following quantities as a function of basis function B_i:

$$\psi_{i,\alpha} = \frac{|J_\alpha|}{2}\int_{-1}^{1} B_i(s,-1)\psi(s,-1)\,ds \tag{8a}$$

$$\psi_{i,\beta} = \frac{|J_\beta|}{2}\int_{-1}^{1} B_i(1,t)\psi(1,t)\,dt \tag{8b}$$

$$\psi_{i,\delta} = \frac{|J_\delta|}{2}\int_{-1}^{1} B_i(s,1)\psi(s,1)\,ds \tag{8c}$$

$$\psi_{i,\gamma} = \frac{|J_\gamma|}{2}\int_{-1}^{1} B_i(-1,t)\psi(-1,t)\,dt \tag{8d}$$

$$\psi_{i,\mu} = \int_{-1}^{1}\int_{-1}^{1} \psi(s,t)\left(\frac{\partial y}{\partial t}\frac{\partial B_i}{\partial s} - \frac{\partial y}{\partial s}\frac{\partial B_i}{\partial t}\right)dsdt \tag{8e}$$

$$\psi_{i,\eta} = \int_{-1}^{1}\int_{-1}^{1} \psi(s,t)\left(\frac{\partial x}{\partial s}\frac{\partial B_i}{\partial t} - \frac{\partial x}{\partial t}\frac{\partial B_i}{\partial s}\right)dsdt \tag{8f}$$

$$\psi_{i,M} = \int_{-1}^{1}\int_{-1}^{1} B_i(s,t)\psi \left|\mathbf{J}\right| \, dsdt \tag{8g}$$

$$S_{i,M} = \int_{-1}^{1}\int_{-1}^{1} B_i(s,t)S(s,t) \left|\mathbf{J}\right| \, dsdt \, . \tag{8h}$$

In Eqs. (8), $\mathbf{J}$ is the Jacobian matrix of the transformation:

$$\mathbf{J} = \begin{bmatrix} \frac{\partial x}{\partial s} & \frac{\partial y}{\partial s} \\ \frac{\partial x}{\partial t} & \frac{\partial y}{\partial t} \end{bmatrix} , \tag{9}$$

$|J_{\alpha,\beta,\delta,\gamma}|$ is the length of physical element side $\alpha,\ \beta,\ \delta,$ or γ, respectively, and $\vec{\Omega}_d = \langle \mu, \eta \rangle$. Additionally, we remind the reader that for a function, $h(x,y)$ the following hold true [6].

$$\int_K h(x,y)dx\, dy = \int_{-1}^{1}\int_{-1}^{1} h(s,t) \left|J(s,t)\right| \, ds\, dt \tag{10}$$

$$\mathbf{J} \begin{bmatrix} \frac{\partial f}{\partial x} \\ \frac{\partial f}{\partial y} \end{bmatrix} = \begin{bmatrix} \frac{\partial f}{\partial s} \\ \frac{\partial f}{\partial t} \end{bmatrix} \tag{11}$$

$$\vec{\nabla}_{xy} h(x,y) = \mathbf{J}^{-1}\vec{\nabla}_{st} h(s,t) \, . \tag{12}$$

Eqs. (7) has more unknowns than equations, requiring the assumption of a solution representation, $\widetilde{\psi}(s,t)$ that approximates the true angular flux solution $\psi(s,t)$.

The UBLD scheme assumes a solution trial space equal to the weight/basis space,

$$\widetilde{\psi}_{UBLD} = \sum_{i=0}^{3} \psi_{i,UBLD} B_i(s,t) \, . \tag{13}$$

Under this assumption, Eqs. (7) becomes a 4×4 linear system of equations. Interested readers are directed to [1] or one of the many other papers that have derived and used UBLD on rectangles and quadrilaterals for a more complete derivation.

The FLBLD [1, 4] alternatively derived as the subcell balance method on quadrilaterals [5] begins with the UBLD equations then lumps (diagonalizes) the UBLD mass and surface matrices. The FLBLD equations are then further manipulated to result in a strictly non-negative solution representation that is second order convergent in space, and is found by solving a 4×4 linear system of equations. Again, the interested reader is directed to [1, 4, 5] for a more detailed derivation.

The BCSZ scheme is defined as being a bilinear function, $\widehat{\psi}_{BCSZ}$,

$$\widehat{\psi}_{BCSZ}(s,t) = \sum_{i=0}^{3} \psi_{i,BCSZ} B_i(s,t) \, , \tag{14}$$

everywhere $\widehat{\psi}_{BCSZ}$, is positive and zero otherwise:

$$\widetilde{\psi}_{BCSZ}(s,t) = \begin{cases} \widehat{\psi}_{BCSZ}(s,t) & \widehat{\psi}_{BCSZ}(s,t) > 0 \\ 0 & \text{otherwise} \end{cases} \, . \tag{15}$$

The initial iterate of $\widehat{\psi}_{BCSZ}$is $\widetilde{\psi}_{UBLD}$. If, and only if, $\widetilde{\psi}_{UBLD} \geq 0$ everywhere within a cell, $\widetilde{\psi}_{BCSZ} = \widetilde{\psi}_{UBLD}$. Using the definition of $\widetilde{\psi}_{BCSZ}$given in Eq. (15) causes Eqs. (7) to be a system of 4 non-linear equations with four fundamental unknowns, $\psi_{i,BCSZ}$ that describe the bilinear function $\widehat{\psi}_{BCSZ}$.

2.1 BCSZ Cell Integration

The definitions of $\psi_{i,\mu},\ \psi_{i,\eta},$ and $\psi_{i,M}$ arising from using $\widetilde{\psi}_{BCSZ}$to close Eqs. (7) require the integration of bivariate polynomials over regions bounded by a bilinear curve. That is to say that given the definition of $\widetilde{\psi}_{BCSZ}$in Eq. (15), the integral contributions to $\psi_{i,\mu},\ \psi_{i,\eta},$ and $\psi_{i,M}$ are non-trivial only over a portion of the cell where $\widehat{\psi}_{BCSZ}(s,t) > 0$. We denote the area where $\widehat{\psi}_{BCSZ} > 0$ as region R. An example layout for is given in Fig. 2. By definition along the dotted

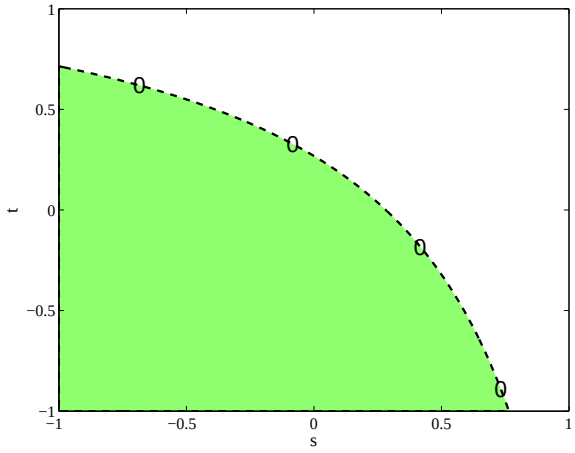

Figure 2. $\widetilde{\psi}_{BCSZ} > 0$ **in green,** $\widetilde{\psi}_{BCSZ} = 0$ **in white, for** $\vec{\psi}_{BCSZ} = [3, -0.5, -1, -0.4]$

line, $\widehat{\psi}_{BCSZ} = 0$. To evaluate $\psi_{i,\mu},\ \psi_{i,\eta},$ and $\psi_{i,M}$ over R, we use a variable limit of integration in either s or t. To do this, we first transform $\widehat{\psi}_{BCSZ}$from an interpolatory polynomial to a moment based polynomial, $f(s,t)$:

$$f(s,t) = f_c + sf_s + tf_t + stf_{st}\,, \tag{16}$$

that we can find using the interpolatory definition of the basis functions:

$$\begin{bmatrix} 1 & -1 & -1 & 1 \\ 1 & 1 & -1 & -1 \\ 1 & 1 & 1 & 1 \\ 1 & -1 & 1 & -1 \end{bmatrix} \begin{bmatrix} f_c \\ f_s \\ f_t \\ f_{st} \end{bmatrix} = \vec{\psi}_{BCSZ}\,, \tag{17}$$

with

$$\vec{\psi}_{BCSZ} = [\psi_{0,BCSZ}, \psi_{1,BCSZ}, \psi_{2,BCSZ}, \psi_{3,BCSZ}]^T\ . \tag{18}$$

Along the dotted line in Fig. 2, $f(s,t) = 0$, and Eq. (16) can be manipulated to find either

- a limit of integration with respect to s, $\bar{l}_s$, that is a function of t , or
- a limit of integration with respect to t, $\hat{l}_t$, that is a function of s:

$$\bar{l}_s = -\frac{f_c + f_t t}{f_s + f_{st} t} \tag{19}$$

$$\hat{l}_t = -\frac{f_c + f_s s}{f_t + f_{st} s}\,. \tag{20}$$

To minimize the amount of computational work that must be performed, we seek a single, generic integrand, for all $\psi_{i,\mu},\ \psi_{i,\eta},$ and $\psi_{i,M}$ quantities. We find this generic integrand by first expanding the specific integrand definitions of $\psi_{i,\mu},\ \psi_{i,\eta},$ and $\psi_{i,M}$ over region R. Starting with the integrand of $\psi_{i,\mu}$

$$\widehat{\psi}_{BCSZ}(s,t)\left(\frac{\partial y}{\partial t}\frac{\partial B_i}{\partial s} - \frac{\partial y}{\partial s}\frac{\partial B_i}{\partial t}\right) = \left[f_c + s f_s + t f_t + st f_{st}\right]\ldots \\ \left(\left[y_{t,c} + s y_{t,s}\right]\left[b_{i,s,c} + t b_{i,s,t}\right] - \left[y_{s,c} + t y_{s,t}\right]\left[b_{i,t,c} + s b_{i,t,s}\right]\right)\,, \tag{21a}$$

then $\psi_{i,\eta}$:

$$\widehat{\psi}_{BCSZ}(s,t)\left(\frac{\partial x}{\partial s}\frac{\partial B_i}{\partial t} - \frac{\partial x}{\partial t}\frac{\partial B_i}{\partial s}\right) = \left[f_c + s f_s + t f_t + st f_{st}\right]\ldots \\ \left(\left[x_{s,c} + t x_{s,t}\right]\left[b_{i,t,c} + s b_{i,t,s}\right] - \left[x_{t,c} + s x_{t,s}\right]\left[b_{i,s,c} + t b_{i,s,t}\right]\right)\,, \tag{21b}$$

and finally $\psi_{i,M}$:

$$B_i(s,t)\widehat{\psi}_{BCSZ}(s,t)\left|J(s,t)\right| = \left[b_{i,c} + s b_{i,s} + t b_{i,t} + st b_{i,st}\right]\left[f_c + s f_s + t f_t + st f_{st}\right]\left[g_c + s g_s + t g_t\right]\,. \tag{21c}$$

In Eqs. (21) we have defined the following:

$$B_i(s,t) = b_{i,c} + s b_{i,s} + t b_{i,t} + st b_{i,st} \tag{22a}$$

$$\frac{\partial B_i}{\partial s} = b_{i,s,c} + t b_{i,s,t} \tag{22b}$$

$$\frac{\partial B_i}{\partial t} = b_{i,t,c} + s b_{i,t,s} \tag{22c}$$

$$\left|\mathbf{J}(s,t)\right| = g_c + s g_s + t g_t \tag{22d}$$

$$\frac{\partial x}{\partial s} = x_{s,c} + t x_{s,t} \tag{22e}$$

$$\frac{\partial x}{\partial t} = x_{t,c} + s x_{t,s} \tag{22f}$$

$$\frac{\partial y}{\partial s} = y_{s,c} + t y_{s,t} \tag{22g}$$

$$\frac{\partial y}{\partial t} = y_{t,c} + s y_{t,s}\,. \tag{22h}$$

Using MATLAB [**?**], each integrand in Eqs. (21) is further expanded, then terms of equal degree bivariate polynomials, $s^m t^n$, with $0 \leq m \leq 3$, $0 \leq n \leq 3$, are collected. This allows us to calculate the twelve separate integrations of $\psi_{i,\mu},\ \psi_{i,\eta},$ and $\psi_{i,M}$, as the multiplication of tweleve unique sets of constants, $\mathbf{C}_{i,\mu}$, $\mathbf{C}_{i,\eta}$, and $\mathbf{C}_{i,M}$, multiplied by the integrations of a single set of bivariate polynomials over R.

2.1.1 Symbolic integration versus numerical integration

Initially, MATLAB [**?**] symbolic algebra generated expressions for the integrations of the generic bivariate polynomials over R were used to evaluate $\psi_{i,\mu},\ \psi_{i,\eta},$ and $\psi_{i,M}$. This worked well at low cell counts, but caused the $\widetilde{\psi}_{BCSZ}$non-linear iteration to fail at higher cell counts. To verify the MATLAB generated expressions, we compared the "exact" symbolic algebra generated results for calculating $\psi_{i,M}$ for $\vec{\psi}_{BCSZ} = [-2\ 0.1\ 200\ 10]^T$ to the value obtained using N_s Gauss quadrature points in s along the curved boundary. A two-point Gauss quadrature in t was used for each corresponding Gauss point in s (tensor product quadrature). An example of the quadrature layout is given in Fig. 3 for $N_s = 4$. In Fig. 4, we plot $E_{i,quad}$, where:

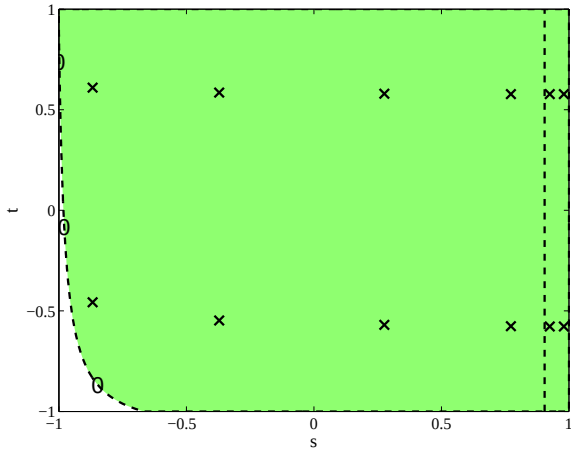

Figure 3. Quadrature point locations for $N_s = 4$ for quadrature integration test.

$$E_i = |\psi_{i,sym} - \psi_{i,num}|\,|\psi_{i,sym}|\,, \tag{23}$$

$\psi_{i,sym}$ is the evaluation of $\psi_{i,M}$ using the symbolic algebra generated expressions, and $\psi_{i,num}$ is the quadrature evaluation of $\psi_{i,M}$ using $2N_s + 4$ quadrature points. Compare the result of Fig. 4 to Fig. **??**, which plots $\widehat{E}_i$:

$$\widehat{E}_i = |\psi_{i,MAX} - \psi_{i,num}|\,|\psi_{i,MAX}|\,, \tag{24}$$

where $\psi_{i,MAX}$ is the quadrature approximation of $\psi_{i,M}$ using Gauss quadrature and $N_S = 40$. It is clear that the "exact" symbolic evaluated expressions suffer from numerical round-off caused by taking the difference of numbers that are of nearly the same magnitude. As such, we now use Gauss-Kronrod [**?**] quadrature to evaluate our bivariate polynomial integrations over R.

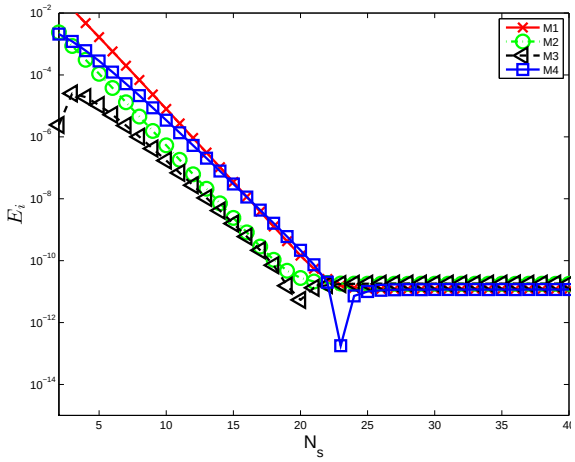

Figure 4. E_i **for quadrature test.**

2.2 BCSZ Edge Integration

3 NUMERICAL RESULTS

4 CONCLUSIONS

5 ACKNOWLEDGMENTS

Portions of this work were funded by the Department of Energy CSGF program, adminstered by the Krell Institute, under grant DE-FG02-97ER25308.

6 REFERENCES

[1] M. L. Adams, "Discontinuous Finite Element Transport Solutions in Thick Diffusive Problems," *Nuclear Science and Engineering*, **137**, pp. 298–333 (2001).

[2] E. D. Fichtl, J. S. Warsa, and J. D. Densmore, "The Newton-Krylov Method Applied to Negative-Flux Fixup in S_N Transport Calculations," *Nuclear Science and Engineering*, **165**, pp. 331–341 (2010).

[3] P. G. Maginot, J. E. Morel, and J. C. Ragusa, "A Non-negative Moment Preserving Spatial Discretization Scheme for the Lienarized Boltzmann Transport Equation in 1-D and 2-D Cartesian Geometries," *Journal of Computational Physics*, **231**, pp. 6801–6826 (2012).

[4] T. A. Wareing, E. W. Larsen, and M. L. Adams, "Diffusion Accelerated Discontinuous Finite Element Schemes for the S_N Equations in Slab and X,Y Geometries," *Proc. International Topical Mtg. on Advances in Mathematics, Computations and Reactor Physics*, Pittsburgh, PA, April 28-May 2, 1991.

[5] M. L. Adams, "Subcell Balance Methods for Radiative Transfer of Arbitrary Grids," *Transport Theory and Statistical Physics*, **26**, pp. 385–431 (1997).

[6] O. C. Zienkiwicz, R. L. Taylor, and J. Z. Zhu, *The Finite Element Method: Its Basis and Fundamentals*, Butterworth-Heinemann, Oxford, United Kingdom (2005).